Coupling between finite element and material point method for problems with extreme deformation

Y.P. Lian, Xiong Zhang,[a)] and Y. Liu
AML, School of Aerospace, Tsinghua University, Beijing 100084, China

(Received 31 December 2011; accepted 10 January 2012; published online 10 March 2012)

Abstract As a Lagrangian meshless method, the material point method (MPM) is suitable for dynamic problems with extreme deformation, but its efficiency and accuracy are not as good as that of the finite element method (FEM) for small deformation problems. Therefore, an algorithm for the coupling of FEM and MPM is proposed to take advantages of both methods. Furthermore, a conversion scheme of elements to particles is developed. Hence, the material domain is first discretized by finite elements, and then distorted elements are automatically converted into MPM particles to avoid element entanglement. The interaction between finite elements and MPM particles is implemented based on the background grid in MPM framework. Numerical results are in good agreement with experimental data and the efficiency of this method is higher than that of both FEM and MPM.
 [doi:10.1063/2.1202103]

Keywords material point method, coupling method, conversion scheme, penetration, landslide

Numerical simulation of problems involving extreme deformation, such as explosion, impact and landslide, is a big challenge for Lagrangian finite element method (FEM) due to the mesh distortion which will decrease its efficiency and accuracy significantly. In contrast to Lagrangian methods, Eulerian methods use Eulerian mesh without mesh distortion but are accompanied by the difficulties for the representation of the boundary of material and tracking the deformation history of material. Additionally, the arbitrary Lagrangian-Eulerian (ALE)[1] formulation is developed to take advantages of both Lagrangian and Eulerian methods but encounters a challenging task to design an efficient and effective mesh-moving algorithm for complicated three-dimensional (3D) problems. Therefore, many researchers focused on the meshless/particle methods to expand the capacity of numerical methods for such problems within the Lagrangian scheme[2–4] during the last several decades, such as the smoothed particle hydrodynamics method (SPH), the element free Galerkin method (EFG), just to name a few. But the efficiency of such methods are lower than that of FEM in each time step and they suffer from their inherent shortcomings. Hence, much effort has been devoted to couple meshless methods with FEM to take advantages of both methods[5–7]. Rabczuk et al. reviewed such work in detail in Ref. 8.

Among meshless methods for such problems, material point method (MPM)[9] takes advantages of both Lagrangian and Eulerian methods. In MPM, the material domain is discretized by a set of Lagrangian particles, which carry all the state variables, such as position, velocity, stress, strain and so on. The momentum equations of particles are solved on a regular Eulerian background grid covering the whole material domain. In each time step, the particles are attached to the background grid so the grid serves as a finite element discretization to the material domain. Unlike other meshless methods, the trial functions of MPM are same as that of FEM. So MPM shows some advantages over other meshless methods in efficiency and tension stability[10]. However, the efficiency of MPM is not as good as that of FEM due to the mappings between background grid and particles, and the accuracy of particles quadrature used in MPM is also lower than that of Gauss points quadrature used in FEM. Hence, Zhang et al.[11] developed an explicit material point finite element method (MPFEM) to take advantages of both FEM and MPM. In MPFEM, the material domain is discretized by finite elements with a predefined background grid in an anticipated large deformation region. If the body moves into the predefined background grid, the element nodes are converted into particles. The limitation of MPFEM is that users are required to identify the potential large deformation region to place the predefined background grid. Furthermore, elements with small deformation are also forced to be converted into particles once they move into the predefined background grid. Recently, Lian and Zhang[12] proposed a coupled finite element material point method based on the contact method, where the body with mild deformation is discretized by FEM and the body with extreme deformation by MPM particles. The interaction between them is implemented based on the contact method via the background grid. But this method does not fully absorb the salient efficiency of FEM either.

To fully take advantages of both FEM and MPM, an adaptive finite element material point (AFEMP) method is proposed in this letter. In AFEMP method, bodies are first discretized by finite elements, and then the distorted elements are adaptively converted into MPM particles based on criteria during the solution process. The interaction between the remaining finite elements and MPM particles is handled based on the background grid in MPM framework. Several numeri-

[a)] Corresponding author. Email: xzhang@tsinghua.edu.cn.

cal examples are presented to validate the efficiency and accuracy of the proposed method.

For a material domain Ω shown in Fig. 1, the momentum equation is given as

$$\nabla \cdot \boldsymbol{\sigma} + \boldsymbol{b} = \rho \ddot{\boldsymbol{u}}, \tag{1}$$

where $\boldsymbol{\sigma}$ is the Cauchy stress, $\boldsymbol{b}$ is the body force per unit volume, ρ is the current density, the superimposed dot indicates the time derivative, and $\boldsymbol{u}$ is the displacement.

For both FEM and MPM, the virtual displacement δu_i is taken as the test function, so the weak form of the momentum Eq. (1) can be given as

$$\int_\Omega \rho \ddot{u}_i \delta u_i \mathrm{d}\Omega + \int_\Omega \sigma_{ij} \delta u_{i,j} \mathrm{d}\Omega - \int_\Omega b_i \delta u_i \mathrm{d}\Omega = 0 \tag{2}$$

As shown in Figs. 1(b) and 1(c), the material domain is discretized by a mesh of elements for FEM, and discretized by a set of particles with a background grid for MPM. In FEM, the mesh is embedded and deforms with the material domain during all time steps. In MPM, the particles are attached to the background grid and deform with it just in one time step and a new background grid is used for the next time step. So in each time step, MPM first maps the state variables of particles to the background grid to establish their momentum equations, and calculates the incremental strain of particles from the velocity field of background grid to update the stress of particles; then, MPM calculates the grid nodal forces by taking the particles as integration points; after that, MPM integrates the momentum equation on the background grid and maps the result of momentum equations back to particles to update their positions and velocities; finally, MPM abandons the deformed background grid.

The MPM can be viewed as a special Lagrangian FEM which employs particles quadrature with remeshing in every time step, so it is straightforward to couple MPM and FEM together. In our coupling scheme, transition nodes are used to connect the FEM domain and MPM domain based on the background grid in MPM framework. As shown in Fig. 2, a material domain is discretized by FEM for its left part and by MPM for the remaining part. The FE nodes located in the interface between two different domains are termed as transition nodes. In order to build connection between FEM domain and MPM, momentum equations of transition nodes are solved on the same background grid by mapping their mass, momentum and nodal force to the background grid abreast with MPM particles. The velocity fields used to calculate the element and particle incremental strains must be identical, so the velocity of the transition nodes must be reset by the velocity field of the background grid. After solving momentum equations on the background grid, the position and velocity of transition nodes are updated from the result of the background grid nodes. Hence the consistency of the displacement and velocity fields between FEM domain and MPM domain is achieved.

A conversion method is proposed here to make the coupling adaptive during the simulation process. In AFEMP method, bodies are firstly discretized by elements. During the simulation process, if one element becomes distortion, it is converted into MPM particles. So there is no need to specify a material domain which is discretized by MPM particles and the accuracy and efficiency salience of finite elements can be retained as long as possible. As shown in Fig. 3, elements A and B are designated as candidates for conversion to particles. In order to keep conservation of mass, momentum and energy during the conversion, one element is converted into four MPM particles whose natural coordinates are taken as $(\pm 0.5, \pm 0.5)$ for their positions calculation. Their velocities are set as those of the adjacent FE nodes. After conversion, the elements A and B and FE node c are deleted, while four particles for each element are added and the FE nodes b, i, d, f, i, g and k are termed as transition nodes. In 3D problems, one hexahedral element is replaced by 8 MPM particles in a similar way.

Using the AFEMP method, we study the tungsten heavy alloys (WHA) long rod projectile penetration experiment conducted by Holmberg et al.[13]. The projectile hits steel armor plate under an angle of 60 degree with initial velocity of 2 500 m/s. The length and the diameter of projectile are 75 mm and 5 mm, respectively, while the size of the target is 150 mm × 150 mm × 9 mm. Johnson Cook model and Gruneisen equation of state are used for both projectile and target. Due to symmetry, half model is used as shown in Fig. 4, which is discretized by hexahedral elements. The projectile's residual length ratios obtained by AFEMP and experiments are 0.72 and 0.76, respectively, while the projectile's residual velocity ratios obtained by AFEMP and experiment are 0.97 and 0.99, respectively. The residual part of the projectile obtained by AFEMP is also in good agreement with the experimental result as shown in Fig. 5. Besides, the computational cost required by AFEMP and MPM are listed in Table 1, which shows that AFEMP is much more efficient than MPM in impact simulation.

Table 1. Computational cost required by MPM and AFEMP

	$\Delta t_{\max}/\mu$s	$\Delta t_{\min}/\mu$s	Steps	CPU/s
MPM	6.45×10^{-2}	3.71×10^{-2}	1 180	2 241
AFEMP	3.67×10^{-2}	1.52×10^{-2}	2 208	838

Another numerical example is a 2D soil collapse experiment conducted by Bui et al.[14], in which many small aluminum bars of diameters 1.0 mm and 1.5 mm were used to model soil collapse. These bars were initially arranged into a rectangular area 200 mm × 100 mm, which was generated by standing two flat solid walls on a flat surface. The experiment was started by quickly removing the right wall horizontally to the one side. Drucker-Prager model is used for the soil. The final shape of

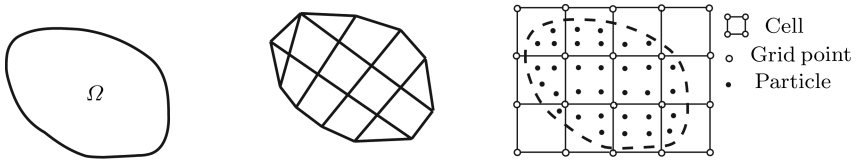

(a) Material domain (b) FEM discretization (c) MPM discretization

Fig. 1. A material domain with different discretization.

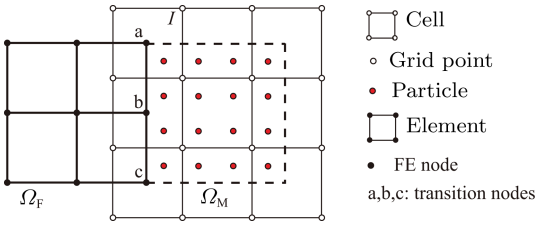

Fig. 2. Coupling between FEM and MPM.

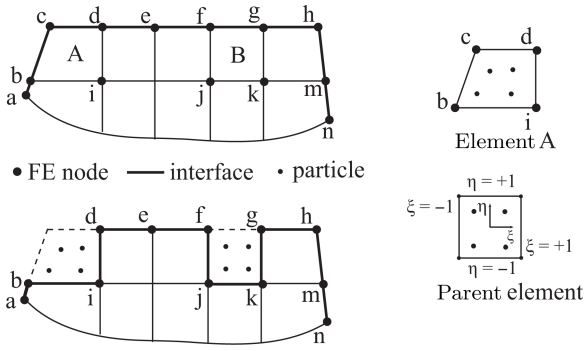

Fig. 3. Conversion of finite elements to particles.

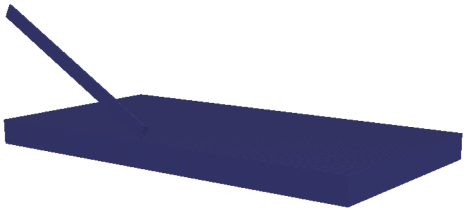

(a) At initial time

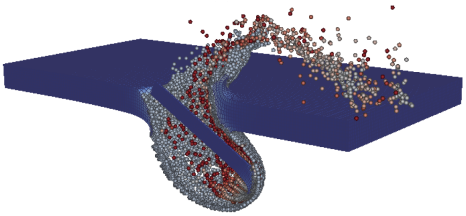

(b) 3.25 μs after impact

Fig. 4. The discretization model for WHA projectile and plate target.

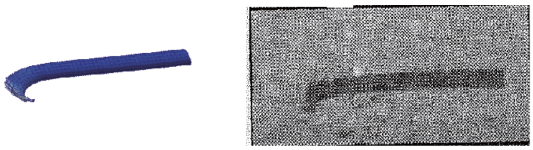

Fig. 5. Comparison of residual part of projectile between numerical result and experimental data.

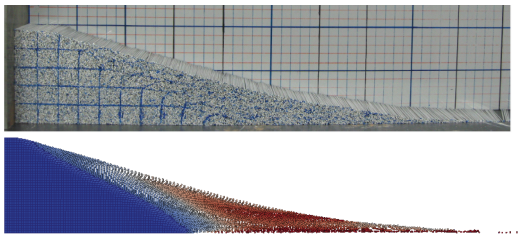

Fig. 6. Final shape of soil obtain by AFEMP and final shape of aluminum bars of experiment.

the soil obtained by AFEMP is compared with the final shape of aluminum bars given by the experiment in Fig. 6, while the surface configurations and failure lines obtained by AFEMP and MPM are compared with experimental results in Fig. 7. Furthermore, the computational cost required by AFEMP and MPM are listed in Table 2 which also shows that AFEMP is much more efficient.

For such dynamic problems with extreme deformation, traditional FEM encounters mesh distortion and element entanglement which will lead to abnormal termination of the simulation. Although MPM can handle large deformation, its efficiency and accuracy are lower than that of FEM for the material domain during the mild deformation period. So FEM and MPM are coupled together in AFEMP method, where FEM are used for the material domain with mild deformation and

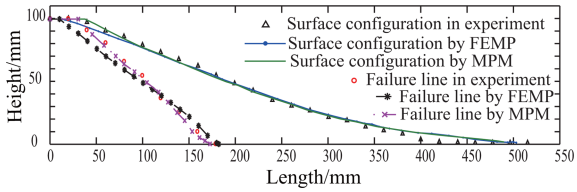

Fig. 7. Final surface configurations and failure lines in experiment and simulation.

Table 2. Computational cost required by MPM and AFEMP

	$\Delta t_{\max}/\mu s$	$\Delta t_{\min}/\mu s$	Steps	CPU/s
MPM	48.41	29.94	34 765	1 791
FEMP	48.41	22.85	47 402	1 123

MPM for the material domain with extreme deformation to inherit the higher efficiency of FEM and capacity of modeling extreme deformation from MPM. Bodies are first discretized by finite elements. A conversion scheme is applied to convert the distortion element into MPM particles adaptively with specified criterion during the simulation process. Hence there is no element distortion in AFEMP which is also suitable for extreme deformation. Furthermore, the efficiency of AFEMP is higher than that of both FEM and MPM as shown in the aforementioned numerical examples.

This work was supported by the National Basic Research Program of China (2010CB832701).

1. W. K. Liu, T. Belytschko, and H. Chang, Comput. Methods Appl. Mech. Engrg. **58**, 227 (1986).
2. T. Belytschko, Y. Krongauz, and D. Organ, et al, Comput. Methods Appl. Mech. Engrg. **139**, 3 (1996).
3. S. Li, and W. K. Liu, Appl. Mech. Rev. **55**, 1 (2002).
4. H. W. Zhang, K. P. Wang, and Z. Chen, Comput. Methods Appl. Mech. Engrg. **198**, 1456 (2009).
5. T. Belytschko, D. Organ, and Y. Krongauz, Comput. Mech. **17**, 186 (1995).
6. G. R. Johnson, Nucl. Eng. Des. **150**, 265 (1994).
7. W. K. Liu, R. A. Uras, and Y. Chen, J. Appl. Mech. **135**, 143 (1997).
8. T. Rabczuk, S.P. Xiao, and M. Sauer, Commun. Numer. Meth. Engng. **22**, 1031 (2006).
9. D. Sulsky, Z. Chen, and H.L. Schreyer, Comput. Methods Appl. Mech. Engrg. **118**, 179 (1994).
10. S. Ma, X. Zhang, and X.M. Qiu, Int. J. Impact Eng. **36**, 272 (2009).
11. X. Zhang, K.Y. Sze, and S. Ma, Int. J. Numer. Meth. Engrg. **66**, 689 (2006).
12. Y. P. Lian, X. Zhang, and Y. Liu, Comput. Methods Appl. Mech. Engrg. **200**, 3482 (2011).
13. L. Holmberg, P. Lundberg, and L. Westerling, In: 14th International Symposium on Ballistics, (1993).
14. H. H. Bui, R. Fukagawa, and K. Sako, et al, Int. J. Numer. Anal. Meth. Geomech **32**, 1537 (2008).